Palaeomonsoon and palaeoproductivity records of $\delta^{18}O$, $\delta^{13}C$ and $CaCO_3$ variations in the northern Indian Ocean sediments

A Sarkar[1,*], R Ramesh[1,†], S K Bhattacharya[1] and N B Price[2]

[1]*Physical Research Laboratory, Ahmedabad 380009, India.*
[2]*Grant Institute of Geology, University of Edinburgh, Edinburgh, EH9 3JW, UK*
**Current address: Indian School of Mines, Dhanbad.*
†*email: ramesh@prl.ernet.in*

$\delta^{18}O$ and $\delta^{13}C$ of *G. sacculifer* have been measured in five cores from the northern Indian Ocean. In addition, high resolution analysis (1 to 2 cm) was performed on one core (SK-20-185) for both $\delta^{18}O$ and $\delta^{13}C$ in five species of planktonic foraminifera. $CaCO_3$ variation was measured in two cores. The results, presented here, show that

- the summer monsoon was weaker during 18 ka and was stronger during 9 ka, relative to modern conditions;
- $\delta^{13}C$ variations are consistent with independent evidence that shows that during the last glacial maximum (LGM; 18 ka) the upwelling was reduced while during 9 ka it was vigorous;
- calculation of $CaCO_3$ flux shows that the LGM was characterized by low biogenic productivity in the Arabian Sea while during the Holocene productivity increased by ∼65%, as a direct consequence of the changes in upwelling. Similar changes (of lesser magnitude) are also seen in the equatorial Indian Ocean. The amount of terrigenous input into the Arabian Sea doubled during LGM possibly due to the higher erosion rate along the west coast.
- $\delta^{18}O$ values indicate that the Arabian Sea was saltier by 1 to 2‰ during LGM. The northern part was dominated by evaporation while in the equatorial part there was an increased precipitation.

1. Introduction

Stable isotope ratios of oxygen ($\delta^{18}O$) and carbon ($\delta^{13}C$) in foraminiferal calcitic tests from ocean sediments have been widely used for palaeoclimatic reconstruction during the Quaternary (Shackleton and Opdyke 1973; Duplessy *et al* 1981; Berger *et al* 1985; Mix 1987; Clemens and Prell 1991; Clemens *et al* 1991; Naidu *et al* 1992; Sirocko *et al* 1993, 1996; Naqvi and Fairbanks 1996; Beufort *et al* 1997; Rostek *et al* 1997). The $\delta^{18}O$ value of the foraminiferal calcite depends on the temperature and $\delta^{18}O$ of the water in which it is formed (Shackleton 1974). Both these parameters exhibit global and regional variations with time. The global components include changes in the sea-surface temperature (SST) and in the distribution of the total water between the world oceans and the continental ice sheets. The regional components depend on variations in SST and $\delta^{18}O$ induced by local upwelling, mixing of water masses and the amount of fresh water discharge near coastal regions. Similarly $\delta^{13}C$ variations in foraminifera have global components like changes in the $\delta^{13}C$ of ΣCO_2 induced by fluctuations in the deep water formation and circulation and in the global productivity due, for instance, to changing wind strengths. The local variations in the input of terrestrial carbon and upwelling also produce a significant effect on the $\delta^{13}C$ of foraminifera. By appropriately assessing and subtract-

Keywords. Oxygen isotopes; carbon isotopes; sediments; foraminifera; productivity; monsoon.

Proc. Indian Acad. Sci. (Earth Planet. Sci.), **109**, No. 1, March 2000, pp. 157–169

ing the global component from the total signal, one can derive information about regional palaeoclimatic changes like the vagaries of the South Asian summer monsoon (Prell 1978; Duplessy 1982; Sarkar *et al* 1990a). Here we report one such study carried out in the Indian Ocean and Arabian Sea based on δ^{13}C and δ^{18}O variations in foraminifera from five sediment cores.

2. Core collection

Core locations and bottom topography are shown in figure 1 and the details are presented in table 1. The cores were collected during two cruises, one each in ORV Sagar Kanya (Cruise # 20) and RRV Charles Darwin (Cruise # 17). An attempt was made to collect the cores from regions with a reasonably flat bottom topography to ensure obtaining continuous and undisturbed climatic records. The two gravity cores SK-20-185 and 186 were sub-sampled at 1 to 2 cm intervals for the top 50 cm and at 5–10 cm intervals for the remaining parts of the cores. The other piston and box cores were sub-sampled at 5 cm intervals.

Table 1. *Description of the sediment cores.*

Core no.	Location Lat./Long.	Water depth (m)	Core length (cm)	Type
SK-20-185*	10°N,71°50′E	2523	300	Gravity core
SK-20-186*	0°N,68°30′E	3564	500	Gravity core
CD-17-30^{+}	19°56'N,61°39′E	3850	800$^{\#}$	Piston core
CD-17-15^{+}	16°38'N,60°39′E	4012	600$^{\#}$	Piston core
CD-17-32^{+}	21°45'N,60°49′E	3150	50	Box core

*SK: Sagar Kanya, an Indian Ship, Department of Ocean Development.
$^{+}$ CD: Charles Darwin, a British Ship, NERC, UK
$^{\#}$ Analysed only up to 300 cm

3. Methods

Sediment samples were soaked in 10% Calgon solution overnight in glass beakers and subsequently washed through a 150 μm sieve with a jet of distilled water. The fraction >150 μm, consisting of adult planktonic foraminiferal tests was oven dried at 60°C. About 30–40 individuals of a given species were picked up under a stereoscopic binocular microscope for isotopic analysis. For the present analyses, foraminiferal tests were chosen from a narrow size range of 250 to 400 mm

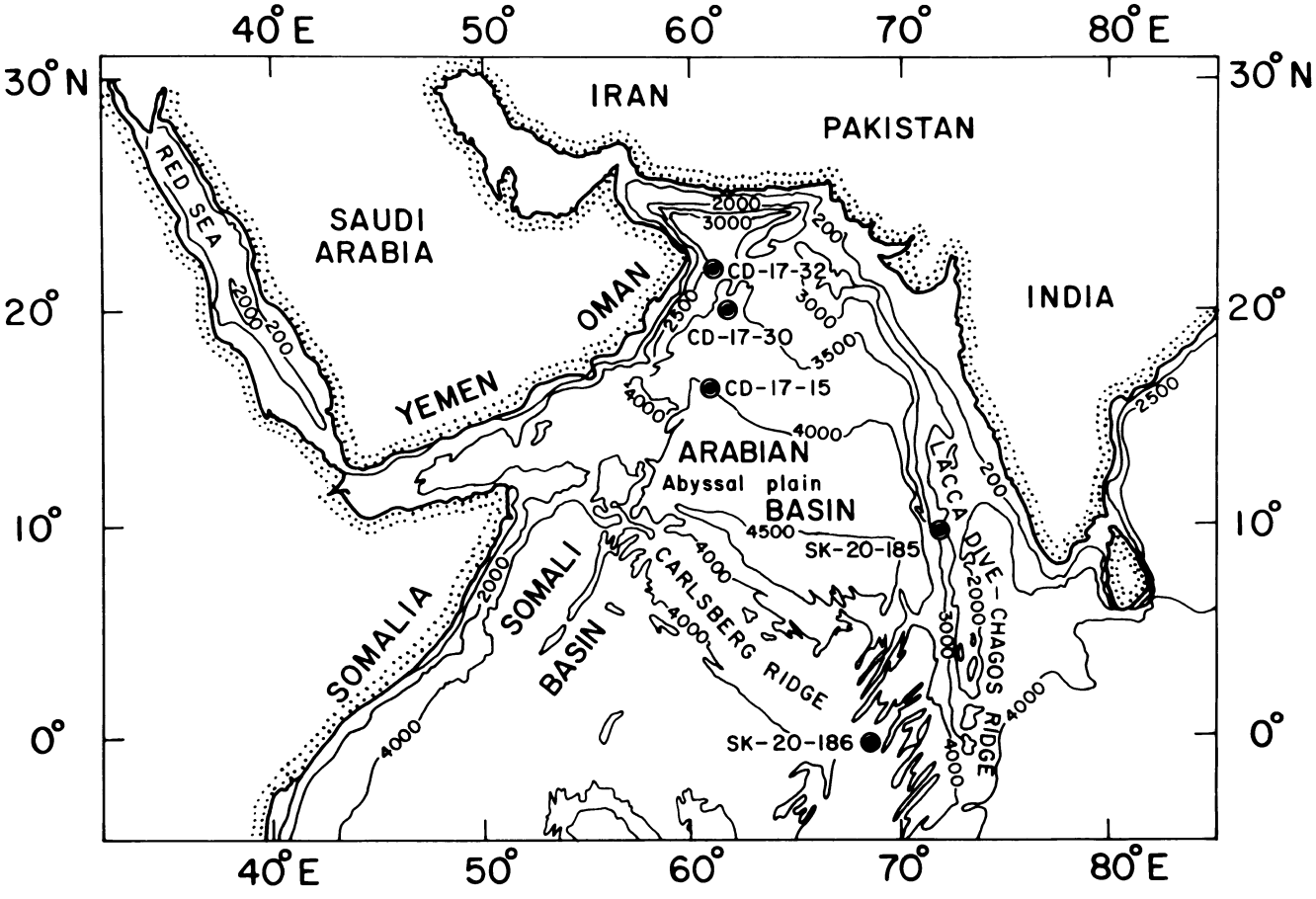

Figure 1. Map of Arabian Sea with depth contours; core locations are shown by dots.

to avoid possible ontogenic effects (Berger *et al* 1985). To remove any adhering extraneous carbonate particles, the samples were given an ultrasonic treatment under distilled water for a few seconds and the water was subsequently absorbed by tissue paper. The samples were dried under vacuum at 150°C for an hour. The details are described elsewhere (Sarkar *et al* 1990b).

The samples were then reacted with 100% H_3PO_4 at 50°C under vacuum in an on-line extraction system (Sarkar and Bhattacharya 1988). Water vapour was removed from the evolved CO_2 gas by passing it through three traps (−100°C). $\delta^{18}O$ and $\delta^{13}C$ were measured in a VG Micromass 602 D mass spectrometer with a precision of ±0.1‰; this is based on replicate measurements of internal laboratory standards ($CaCO_3$), Z-Carrara and Marble V, kindly provided by N. J. Shackleton of the Cambridge University. All the samples were run at least in duplicate. The mean intra-sample variability for 300 such duplicate analyses is ±0.15‰ and the data presented in this paper are mean values of duplicates relative to V-PDB standard.

In addition to stable isotope ratios, the $CaCO_3$ content was measured in two cores as a function of depth. About 100 mg of the bulk sediment was subjected to a 2% acetic acid leaching in batches, centrifuged and the clear solution was made to 100 ml and titrated against 0.01 M standardized EDTA. The reproducibility of $CaCO_3$ measurement, estimated from replicate analyses of both standard carbonate and samples is ±1%. Three sediment cores were also dated by ^{14}C, U-Th methods (Sarkar *et al* 1992). Details of the procedures are reported elsewhere (Sarkar 1989). The dates refer to uncorrected radiocarbon ages and are *not calendar ages*.

4. Results and discussion

4.1 *Sedimentation rates*

The sedimentation rates of three cores SK-20-185, SK-20-186 and CD-17-30 based on ^{14}C and U-Th methods are presented in table 2. SK-20-185 has a uniform sedimentation rate during the last 25 ka while in SK-20-186, there is a break at 22–23 cm depth. The sedimentation rate during the last glacial period in the latter core is 0.6 cm/ka, a factor of 4 less than the Holocene rate. CD-17-30 has a higher sedimentation rate due to higher biological productivity in the upwelling zone of the western Arabian Sea and a much higher terrigenous accumulation. ^{230}Th-based sedimentation rates, where available, agree well with those based on the ^{14}C methods within experimental uncertainties. The details are published elsewhere (Sarkar *et al* 1992).

Table 2. *Sedimentation rates by various methods*

Core	Method	Sedimentation rate (cm/kyr)
SK-20-185	^{14}C	2.2±0.1 (up to 70 cm)
	^{230}Th (excess)	2.5±0.5 (up to 145 cm)
SK-20-186	^{14}C	2.4±0.1 (0 to 23 cm)
		0.6±0.1 (below 23 cm)
	^{230}Th (excess)	0.6±0.1 (up to 147 cm)
CD-17-30	^{14}C	7.7±0.6 (up to 185 cm)

After the retrieval of gravity cores SK-20-185 and SK-20-186, the top parts in both were found to be disturbed by the coring operation and a small portion of the surface was slumped. Considering the cross sectional area of the corer and the weight of the material slumped, the length of the sediment disturbed was found to be 1 to 2 cm, taking the density to be about 0.7 gm/ml (for top parts) in both the above cores. [This material, with the overlying water in the core spread to a distance of 15 cm and Naidu *et al* (1989), who shared these cores with us for studying foraminiferal assemblages, assumed this length (15 cm) of the core top to be disturbed]. The depth assignments have been made after making due correction for this slumping. These disturbed sediments in SK-20-185 and SK-20-186 have a ^{14}C age of 4.0 ± 0.1 ka and 5.2 ± 0.1 ka respectively. Such core top ages are typical of cores with bioturbation, but these datings show the surface sediments to be of Holocene age.

4.2 *Modern oceanographic conditions*

The present day oceanographic condition over the Arabian Sea is dominantly controlled by seasonally varying insolation and wind system, which cause both monsoonal rain over the Indian region and intense upwelling in the western Arabian Sea. Freshwater discharge through the peninsular rain-fed rivers into the southeast Arabian Sea, coupled with a strong evaporation in the northern sector controls the salinity pattern which increases from 35‰ to 36.5‰ (Wyrtki 1971). During the summer a pronounced temperature drop of about 4°C takes place along the Somali and Arabian coasts, due to upwelling induced by the monsoon circulation. This has been discussed in detail by Wyrtki (1973) and Duplessy (1982).

4.3 *Isotopic composition of core-top foraminifera*

Using GEOSECS (Gote-Ostlund *et al* 1987) surface water $\delta^{18}O$ values and mean annual SST data (Wyrtki 1971), equilibrium calcite $\delta^{18}O$ values have been calculated for the five core locations, CD-17-15, CD-17-30, CD-17-32, SK-20-185 and SK-20-186. These values are in good agreement with the measured core top *G. sacculifer* $\delta^{18}O$ values (table 3), except for SK-20-186. There are no $\delta^{18}O$ data for this station and the

Table 3. *$\delta^{18}0$, $\delta^{13}C$ values of calcite* and the observed values of core top G. sacculifer* (250–400 μm).

Core No	Mean Annual SST(°C)	$\delta^{18}O^1$ Calc. (‰) PDB	$\delta^{18}O^2$ Gs (‰) PDB	$\delta^{13}C^3$ Calc. (‰) PDB	$\delta^{13}C^4$Gs (‰) PDB	$\Delta^{18}O^5$ (‰)	$\Delta^{13}C^6$ (‰)
CD-17-32	24.5	−1.1	−1.22	3.78	1.11	0.12	2.67
CD-17-30	25.5	−1.32	−1.28	3.81	1.35	−0.04	2.46
CD-17-15	26.0	−1.43	−1.43	3.83	1.27	0.0	2.56
SK-20-185	27.5	−1.73	−1.72	3.77	1.76	−0.01	2.01
SK-20-186	28.5	−1.94	−1.39	3.91	1.79	−0.55	2.12

* Calculated using equations (Shackleton 1974 and Emrich *et al* 1970).
[1] δ^{18}O values, for all the 5 core locations are calculated, taking surface δ^{18}O of water as 0.56‰ (PDB), station 416, GEOSECS 1987.
[2,4] δ^{18}O and δ^{13}C values of core top *G. sacculifer* (250–400 μm) respectively.
[3] δ^{13}C values are calculated based on bicarbonate-δ^{13}C data of GEOSECS (Gote-Ostlund et al 1987). For first 3 core locations, data from closest location i.e. station 416 are used. For the other two (185 and 186) cores, values of stations 417 and 418 are used respectively.
[5,6] Difference in δ^{18}O and δ^{13}C between calculated and observed core top δ values respectively.

assumed δ^{18}O value of 0.56 (relative to CO_2-PDB) for surface water may be incorrect. Even so, we believe that our data in general, indicate that *G. sacculifer* grows in oxygen isotopic equilibrium at least for the 250 to 400 mm size range, confirming earlier results (Erez and Luz 1983). This species has thus been preferred for analysis in the other cores.

Contrary to this, the δ^{13}C values of core-top *G. sacculifer* show a depletion of about 2‰ or more (table 3) relative to calculated equilibrium values. Carbon isotopic ratios are known to deviate from the equilibrium values (Duplessy *et al* 1981) but the offset is assumed to be constant with time and does not affect the glacial-interglacial differences in δ^{13}C (Kallel *et al* 1988).

4.4 *Oxygen isotopes as a function of time*

δ^{18}O values for five species of foraminifera in SK-20-185 are shown in table 4(a) (high resolution) and for *G. sacculifer* alone (lower resolution, same core) are presented in table 4(b). Data for the other four cores are presented in tables 5 and 6 and in figure 2. Data from CD-17-32 are not plotted as this core does not reach the last glacial maximum (LGM). In SK-20-185 there is a negative spike of about 1‰ at LGM (i.e. 28–34 cm), which possibly represents the enhancement of the winter monsoon current (Sarkar *et al* 1990a, see discussion at the end of this section), and is not shown in figure 2. Core CD-17-30 has a sedimentation rate of 7.7 cm/ka (^{14}C based) and has been analysed up to

Table 4(a). *Oxygen and carbon isotope data on core SK-20-185. High resolution analysis on 5 species*.*

Depth (cm)	δ^{18}O (‰)					δ^{13}C (‰)					$CaCO_3$ (‰)
	1	2	3	4	5	1	2	3	4	5	
2.50	−1.34	−1.87	−1.49	–	−0.81	1.74	1.43	1.94	–	1.37	67.5
4.50	−1.72	−2.24	−1.61	−0.94	−0.82	1.76	1.32	1.80	0.60	1.37	65.8
6.50	−1.70	−2.23	−1.44	−0.96	−1.02	1.53	1.27	1.50	0.58	1.34	–
8.50	−1.41	−1.90	−1.38	−1.04	−0.74	1.53	1.01	1.61	0.59	1.16	–
10.50	−1.17	−1.89	−0.69	−0.58	−0.21	1.42	1.25	1.62	0.57	1.21	60.3
12.50	−0.60	−1.17	−0.63	−0.11	−0.15	1.50	1.17	1.21	0.50	1.47	–
14.50	−0.94	−1.45	−0.52	−0.04	−0.52	1.31	0.90	1.34	0.59	1.13	52.6
16.00	−0.46	−1.37	−0.01	0.12	−0.04	1.05	0.84	1.45	0.65	1.36	51.6
18.00	−0.16	−0.61	−0.08	0.55	0.64	1.50	1.17	1.44	0.65	1.39	48.1
20.00	−0.16	−1.21	−0.12	0.82	0.15	1.36	0.96	1.51	0.67	1.48	–
22.00	−0.09	−0.72	0.38	1.03	0.51	1.48	1.11	1.43	0.92	1.53	–
24.00	0.08	−0.48	0.38	0.85	0.78	1.49	1.21	1.47	0.62	1.61	42.6
26.00	0.23	−0.21	0.43	1.13	0.87	1.40	1.19	1.35	0.76	1.63	–
28.00	−0.14	−0.42	0.23	1.13	0.59	1.54	1.30	1.47	0.76	1.57	–
30.00	−0.30	−0.53	0.31	0.95	0.87	1.36	1.24	1.71	0.70	1.70	41.0
32.00	−0.97	−0.75	0.05	0.95	0.40	1.66	1.21	1.72	0.70	1.42	–
34.00	−0.88	−0.67	−0.69	–	0.65	1.62	1.23	1.66	–	1.65	–
37.50	0.34	−0.28	0.65	–	0.80	1.54	1.04	1.58	–	1.71	40.2
42.50	0.26	−0.42	0.20	–	0.57	1.73	1.26	2.01	–	1.62	–
47.50	0.26	−0.63	0.22	–	0.79	1.65	0.85	1.94	–	1.54	38.5

(1) *G. sacculifer* (250–400 μm); **(2)** *G. ruber* (250–355 μm); **(3)** *O. universa* (400–500 μm); **(4)** *P. obliquiloculata* (250–400 μm); **(5)** *G. menardii* (250–400 μm); * (30–40) individuals per aliquot.

Table 4(b). *Oxygen and carbon isotope data on core SK-20-185. Analysis on G. sacculifer at larger intervals.*

Depth (cm)	δ^{18}O (‰)	δ^{13}C (‰)	$CaCO_3$ (%)	Depth (cm)	δ^{18}O (‰)	δ^{13}C (‰)	$CaCO_3$ (%)
52.50	0.40	1.92	–	147.50	−0.30	1.65	37.4
57.50	0.22	1.88	40.2	152.50	−0.24	1.32	32.6
62.50	0.11	1.83	40.2	157.50	−0.12	1.46	31.4
67.50	−0.02	1.84	42.8	162.50	−0.44	1.52	32.6
72.50	−0.25	1.79	45.2	167.50	−0.68	1.50	28.6
77.50	−0.17	1.69	44.4	172.50	−0.34	1.41	32.5
82.50	−0.48	1.65	46.7	177.50	−0.90	1.36	35.2
87.50	−0.06	1.74	45.6	182.50	−0.90	1.36	33.0
92.50	−0.23	1.53	-	190.00	−0.51	1.53	44.0
97.50	−0.21	1.71	45.7	200.00	−0.80	1.63	48.6
102.50	−0.44	1.62	46.1	210.00	−1.09	1.87	53.5
107.50	−0.21	1.75	-	220.00	−0.60	1.82	42.7
112.50	−0.67	1.50	42.9	230.00	−0.87	1.42	56.0
117.50	−0.53	1.42	45.4	240.00	−0.89	1.47	59.4
122.50	−0.49	1.48	-	250.00	−1.05	1.48	55.1
132.50	−0.32	1.47	43.4	260.00	−1.18	1.76	52.1
137.50	−0.14	1.54	45.8	270.00	−1.10	1.71	49.7
142.50	−0.07	1.49	41.4	280.00	−1.13	1.45	49.2
–	–	–	–	290.00	−0.84	1.55	51.0

Table 5. *Oxygen and carbon isotope data* on cores from Charles Darwin cruise.*

	CD 17-30			CD 17-15			CD 17-32	
Depth (cm)	$\delta^{18}O_{PDB}$ (‰)	$\delta^{13}C_{PDB}$ (‰)	Depth (cm)	$\delta^{18}O_{PDB}$ (‰)	$\delta^{13}C_{PDB}$ (‰)	Depth (cm)	$\delta^{18}O_{PDB}$ (‰)	$\delta^{13}C_{PDB}$ (‰)
5.0	−1.28	1.35	47.5$^{\#}$	−1.43	1.27	5.0	−1.22	1.11
15.0	−1.21	1.13	–	–	–	15.0	−1.05	1.12
25.0	−0.61	1.21	–	–	–	25.0	−0.65	1.22
42.5	−0.36	1.14	0.0^{+}	−0.08	0.81	32.0	−1.11	1.29
50.0	0.21	1.36	1.0	0.73	1.18	41.0	−0.89	1.13
55.0	0.14	1.06	11.0	0.76	1.11	49.0	−0.95	1.31
65.0	0.87	1.13	20.5	0.52	1.00			
75.0	0.69	1.07	26.5	−0.35	0.83			
85.0	0.87	1.34	37.5	0.34	0.95			
92.5	0.28	0.82	47.5	0.65	1.07			
100.0	0.61	1.27	57.5	0.89	0.88			
112.5	0.35	0.95	67.5	0.47	0.91			
130.0	1.01	1.13	77.5	0.90	0.64			
150.0	0.90	0.90	112.5	0.32	1.03			
165.0	1.03	1.17	127.5	0.61	1.20			
195.0	0.74	1.22	142.5	0.17	0.77			
212.5	0.42	1.02	157.5	0.19	0.93			
235.0	0.58	1.02	175.0	−0.51	0.98			
250.0	0.52	1.13	182.5	0.19	0.73			
262.5	0.26	0.86	205.0	0.23	0.93			
277.5	0.18	0.64	227.5	0.50	0.91			
307.5	0.15	0.78	262.5	−0.49	0.20			
–	–	–	297.5	0.41	1.15			

* Measured on *G. sacculifer* (250–400 μm) with 30–40 individuals per aliquot.
$^{\#}$ Box core (foraminifera absent above this depth).$^{+}$Piston core, disturbed top.

isotope-stage-3. SK-20-185 has a mean sedimentation rate of 2.2 cm/ka and extends up to stage-5e. SK-20-186 has a long climatic record ending at stage-11. Bold arrows in these three cores indicate the 18 ka LGM level (based on ^{14}C dates). The different stage allotments have been done in comparison with SPECMAP data (Imbrie *et al* 1984). The timing of various isotope stages, calculated using ^{14}C data for the top part of core SK-20-185 agrees well with those of the SPECMAP data. This indicates that the sedimentation rate (estimated from the top part of this core) was relatively constant throughout. This is not true in the case of SK-20-186; the extrapolated ^{14}C ages disagree with SPECMAP data. The variation in sedimentation rate here is indicated by the ^{14}C data during the last 40 ka (table 2).

CD-17-15 (piston core) does not yield a good δ^{18}O stratigraphy. The core-top δ^{18}O value is 0.08‰

Table 6. *$CaCO_3$, oxygen and carbon isotope data (G. sacculifer,* 250–400μm, 30–40 tests)on core SK-20-186.

Depth (cm)	$\delta^{18}O$ (‰)	$\delta^{13}C$ (‰)	$CaCO_3$ (%)	Depth (cm)	$\delta^{18}O$ ‰	$\delta^{13}C$ ‰	$CaCO_3$ (%)	Depth (cm)	$\delta^{18}O$ (‰)	$\delta^{13}C$ (‰)	$CaCO_3$ (‰)
1.00	−1.37	1.67	–	94.5	−0.07	1.48	81.6	257.0	−0.66	1.33	88.3
2.50	−1.39	1.79	87.8	104.5	0.01	1.43	80.4	267.00	−0.78	1.33	85.8
11.50	−1.10	1.68	87.9	114.5	0.00	1.39	79.9	277.00	0.06	1.21	85.8
13.50	−0.85	1.71	82.0	124.5	−0.21	1.49	86.2	287.00	0.12	1.49	83.3
15.50	−0.51	1.74	83.3	129.5	−0.35	1.32	83.2	297.00	−0.48	1.37	84.0
17.50	−0.49	1.76	84.3	134.5	−0.61	1.45	82.3	307.00	−0.47	1.38	83.5
19.50	−0.57	1.82	82.5	139.5	−0.42	1.46	84.1	317.00	0.31	1.44	83.3
21.50	−0.47	1.78	81.8	144.5	−0.5	1.54	84.9	327.00	0.21	1.60	83.4
24.50	−0.32	1.65	82.5	149.5	−0.52	1.71	87.0	337.00	0.13	1.72	83.7
26.50	0.00	1.99	82.2	154.5	−0.75	1.55	86.2	347.00	0.05	1.64	82.8
28.50	0.13	1.84	82.0	159.5	−0.60	1.48	86.9	357.00	−0.38	1.65	83.5
30.50	−0.30	1.73	81.3	164.5	−0.54	1.53	83.8	367.00	−0.59	1.45	85.6
32.50	−0.31	1.76	83.7	169.5	−0.35	1.51	83.1	377.00	−0.40	1.62	88.9
43.00	−0.37	1.78	79.5	174.5	−0.40	1.64	86.7	387.00	−0.03	1.42	81.5
47.00	−0.46	1.79	80.9	179.5	−0.60	1.51	86.2	397.00	−0.22	1.56	85.5
53.00	−0.83	1.68	82.3	184.5	−0.90	1.46	85.1	407.00	−0.73	1.41	87.1
57.00	−0.70	1.91	85.1	189.5	−0.62	1.46	86.1	417.00	−0.46	1.53	86.4
64.50	−0.68	1.70	85.6	197.5	−0.43	1.44	84.1	427.00	−0.28	1.37	87.5
69.50	−0.84	1.57	83.6	207.00	−0.18	1.31	83.4	437.00	−0.47	1.46	86.5
74.50	−0.92	1.62	84.2	217.00	−0.13	1.38	82.8	447.00	−0.27	1.45	86.7
79.50	−0.71	1.42	83.2	227.00	−0.39	1.67	83.4	457.00	−0.45	1.27	87.1
84.50	−1.00	1.29	85.1	237.00	−0.41	1.54	87.5	467.00	−0.69	1.43	87.9
89.50	−0.70	1.24	79.6	247.00	−0.56	1.52	88.6	477.00	0.01	1.26	88.7
								487.00	0.43	1.15	84.1

(compare with other core-top $\delta^{18}O$ values in the nearby cores) and an erratic excursion of $\delta^{18}O$ is seen (figure 2) all through the 300 cm analysed. This reflects the slumped nature of the sediments, consistent with the litholog showing distinct turbidite layers.

The Holocene-LGM amplitudes in SK-20-185 and CD-17-30 are 2.12 and 2.28‰ respectively. For SK-20-185 Holocene (most depleted $\delta^{18}O$) depth is taken to be 4.5 cm and LGM (based on ^{14}C age) depth to be 31.0 cm; for CD-17-30 Holocene depth is taken to be 5.0 cm and LGM depth to be 100 cm. Considering the glacial ice volume effect to be 1.6‰ (Imbrie *et al* 1984), these large amplitudes in the Arabian Sea core show an extra 0.5 to 0.7‰ effect, which is local in nature. Such an enrichment in both the northern and southern cores during LGM indicates that most of the Arabian Sea is likely to have been more saline than today by about 1 to 2‰ [we use the data of Duplessy *et al* (1981) to calculate that for a 1‰ change in salinity, $\delta^{18}O$ changes by about 0.33‰]. We ascribe this to a lesser fresh water run off into the Arabian Sea, because of a weakened summer monsoon during LGM. The Holocene difference in $\delta^{18}O$ between these two locations (∼0.4‰) is slightly smaller than the LGM difference (∼0.6‰), thus making the respective total amplitudes (2.12 and 2.28‰) slightly different. This could be due to a stronger evaporation in the northern Arabian Sea compared to the southern Arabian Sea. This differential rate of evaporation was probably strong enough to compensate the effect of warming in the north due to reduced upwelling because of the weaker summer monsoon.

In the equatorial Indian Ocean, the Holocene-LGM $\delta^{18}O$ amplitude (SK-20-186) is only 1.5‰ An increased precipitation over the equatorial Indian Ocean during LGM could have been responsible for such a reduced amplitude. The above findings confirm the earlier work of Duplessy (1982). Alternatively, a smaller ice volume effect (1.1‰ contrary to 1.6‰, Labeyrie *et al* 1987) coupled with a 2°C reduction in SST could have produced such an amplitude.

In the beginning of this section we referred to a negative excursion of about 1‰ in the oxygen isotopic composition of three planktonic foraminifera in core SK-20-185 from the Arabian Sea during LGM. We interpreted this as the combined effect of sea surface warming due to a weaker southwest monsoon and an enhanced northeast monsoon (Sarkar *et al* 1990a). Krishnamurthy (1990) and Gupta *et al* (1992) have questioned this since the river discharge from peninsular India, according to them, is only 13% during winter, from modern river discharge data. They have ignored two major rivers, Cauvery and Pennar and also fail to note that during winter there are frequent cyclones in the Bay of Bengal which bring enormous amounts of rain to the east coast of India causing loss of life and property. We had proposed that as the northeast monsoon became stronger during LGM (Duplessy 1982; Van Campo *et al* 1982), the frequency of such flooding events must have increased (Sarkar *et al* 1990a). Krishnamurthy (1990) and Gupta *et al*

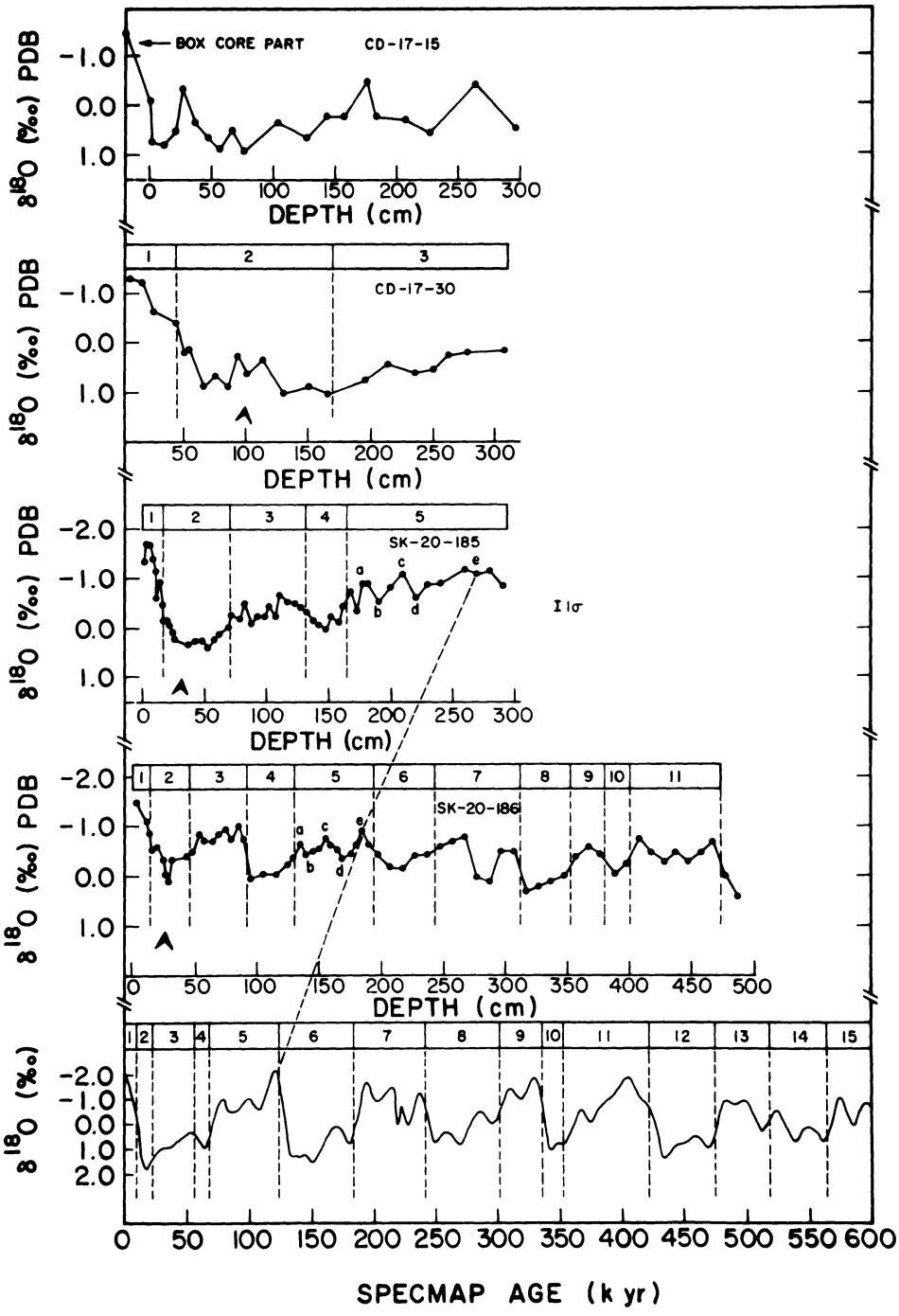

Figure 2. Oxygen isotope data of *G. sacculifer* from cores CD 17-15, CD 17-30, SK 20-185, SK 20-186 and SPECMAP for comparison.

(1992) have overlooked this aspect. Further, modern river discharge is regulated by many dams giving a low flux value not applicable during LGM. Duplessy's (1982) data also support our contention; salinity contours which run east-west today due to fresh water discharge from the Ganges and Brahmaputra in the north, ran north-south due to a reduction in such discharge due to the weakening of the southwest monsoon and probable enhancement in the discharge from the peninsular rivers, which drained vast amounts of coastal precipitation during floods.

The alternative mechanisms proposed by Krishnamurthy (1990) and Gupta *et al* (1992) do not stand scrutiny. Krishnamurthy conjectured that the seasonal abundances of *G. ruber* and *G. sacculifer* peak respectively during summer and late summer early autumn, whereas the available plankton tow data (Guptha *et al* 1990) do not support this. Gupta *et al* (1992) propose that the negative excursion was caused by warming and consequent melting of the Tibetan ice sheet [based on *incorrect* plotting of data lifted from the thesis of Sarkar (1989), as confessed later by

Gupta and Sharma (1993) in reply to a note by Naqvi (1993)]. This is contrary to Broecker and Denton's (1989) observation that during LGM, the equilibrium line altitude of glaciers (including tropical high altitude ones) was considerably lower in both the hemispheres. Further, there is no evidence for an ice sheet in the Himalaya during LGM (Benn and Owen 1998). Gupta *et al* (1992) quote two observations to support their view: (i) Increased abundance of *Juniperus* pollen during LGM in Tsokar Lake, Ladakh (Bhattacharyya 1989) and (ii) Oxygen isotope data from the Dunde ice cap (Thompson *et al* 1989). The former could be due either to changes in the wind pattern and consequent change in the source of pollen to the lake or due to enhanced precipitation from the western disturbance, which brings rain to the dry Ladakh region during winters. The latter has a number of problems. Cole *et al* (1991) have measured the stable isotope ratios in the Dunde ice cap and show that the oxygen isotopic record is complex and does not depend on temperature in the usual sense. They also suggest that changes in the source and direction of air masses are mainly responsible for the observed isotopic variations. Similar conclusions were reached by Pande *et al* (in press) for the isotopic composition of precipitation in Ladakh Himalaya. Finally Gupta *et al's* crude model which aims to calculate the required increase in the northeast monsoon to explain the negative spike has major flaws. They assume the top 100 m of the Bay of Bengal to be laterally well mixed. This is incorrect as even today we can see a salinity gradient, 30 per mil in the north to 35 per mil in the south. Furthermore the transport of low salinity water from the Bay of Bengal to the Arabian Sea takes place through an ocean current, limited in dimensions. Gupta *et al* ignore this fact and by mixing up everything, they "show" that a factor of 10 increase in the northeast monsoon precipitation is required. In view of the above such a large increase is not needed to explain 1 per mil negative excursion.

4.5 *Carbon isotopes*

Phytoplanktons preferentially fix more ^{12}C than ^{13}C of the available carbon within the euphotic zone of the ocean. As a result, phytoplankton $\delta^{13}C$ is depleted (-20 to -26‰) and CO_2 of the surface ocean becomes enriched ($+2$‰) (Kroopnick 1985). Oxidation of this organic matter in the deeper water produces a depleted $\delta^{13}C$ of the ΣCO_2. Local effects like up-welling alter the $\delta^{13}C$ profiles of the water column. Changes in productivity and upwelling are therefore likely to be recorded in the $\delta^{13}C$ planktonic foraminifera.

$\delta^{13}C$ values of *G. sacculifer* in the five cores are presented in tables 4(a), 4(b), 5 and 6. In SK-20-185, four other species of planktic foraminifera have been analysed in addition to *G. sacculifer*. These species have different depth habitats and part of this core was analysed with a high resolution of 1 to 2 cm from surface to the glacial level. A plot of $\delta^{13}C$ with depth is shown in figure 3 for the four species. Early Holocene (~9 ka) and glacial (~20 ka) periods are indicated by bold arrows. The three species *G. sacculifer*, *G. ruber* and *O. universa* show more or less similar variations. A 5-point moving average (dashed line) has been calculated to smooth out the data, which reveals the following features:

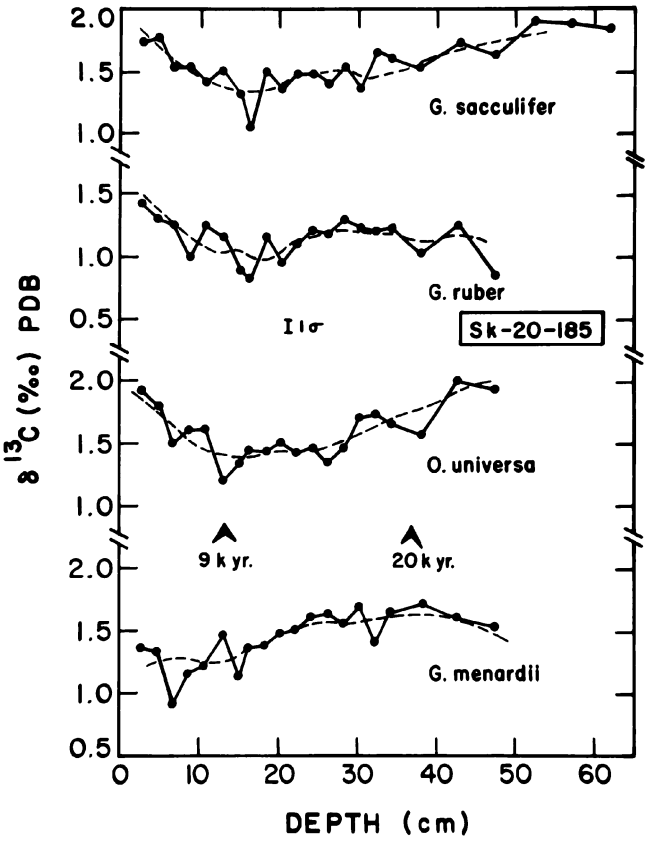

Figure 3. Carbon isotope data for four species in SK 20 -185.

- Around 9 ka, there are $\delta^{13}C$ minima in *G. sacculifer*, *G. ruber* and *O. universa*. The magnitudes of these minima, relative to the surface values, is about 0.5 ± 0.1‰.
- Relative to 9 ka, glacial $\delta^{13}C$ values in these species show an enrichment by 0.2‰ (*G. ruber*) to 0.6‰ (*O. universa*).
- *G. menardii* does not show a significant difference between surface and 9 ka levels. However, the glacial value is enriched relative to surface by about 0.4‰.
- *P. obliquiloculata* (not shown in figure 3) has near constant $\delta^{13}C$ ($\sim 0.66 \pm 0.1$‰) values throughout this length (2 to 48 cm).
- Down-core variations in $\delta^{13}C$ of *G. sacculifer* are positively correlated with those of *G. ruber* and *O. universa* (figure 3), both with a correlation coefficient of 0.6, significant at 2.5% level.

The present day value of $\delta^{13}C$ of dissolved CO_2 in the Arabian Sea surface water is 1.6 to 1.8‰, while deeper (100 to 200 m) waters have a value of 0 to 0.3‰ (Gote-Ostlund *et al* 1987). Mixing of the upwelled water with the surface could produce a depletion in the surface water $\delta^{13}C$ by a maximum of 1.5‰. On the other hand, the surface productivity is linked to the upwelling, that brings nutrients from the deeper layers. An increased upwelling will enhance productivity which in turn will enrich the $\delta^{13}C$ of surface water CO_2 and hence that of the planktonic foraminifera. Therefore, the resultant change in the surface water $\delta^{13}C$ is dependent on which of these two effects (mixing with $\delta^{13}C$ depleted deeper water due to upwelling on the one hand and enhanced productivity on the other) is stronger.

Independent evidence shows that during LGM, the summer monsoon was weaker than today (Nair and Hashimi 1980; Prell 1984; Sarkar *et al* 1990a); upwelling was weaker and consequently the productivity reduced. The surface dwelling planktonic foraminifera analysed by us show a ^{13}C enrichment of 0.2 to 0.6‰ during LGM, consistent with the effect of weaker upwelling. They also show a depletion of about 0.5‰ during 9 ka, consistent with an enhanced summer monsoon activity and a stronger upwelling.

G. menardii shows only a 0.4‰ enrichment in ^{13}C during LGM; it shows no significant change between 9 ka and the present. This is probably because of the deeper habitat of this species (Duplessy 1982). With lower productivity during LGM, the deeper waters would have been relatively enriched in $\delta^{13}C$ because of the reduced supply of organic matter from the top. *P. obliquiloculata* (with the most depleted $\delta^{13}C$) has the deepest habitat (∼100 m) and is not affected by the change in the $\delta^{13}C$ gradient in the upper water column; therefore it does not exhibit any significant variation during the last 25 ka.

$\delta^{13}C$ values for *G. sacculifer* are shown in figures 4 and 5 for cores SK-20-186, CD-17-30 and CO-17-15. The $\delta^{13}C$ minimum around 9 ka (as found in SK-20-185) is not present in these cores. Whereas SK-20-186 is far away from any coastal upwelling regime and is not expected to show a temporal change in $\delta^{13}C$, CD-17-30 is clearly within the upwelling centre off Arabia. This core does not show the $\delta^{13}C$ change probably because the productivity is so high that the corresponding enrichment in $\delta^{13}C$ balances the effect of vertical mixing. Prell and Curry (1981) have observed that core top foraminifera across this upwelling zone do not record any $\delta^{13}C$ change.

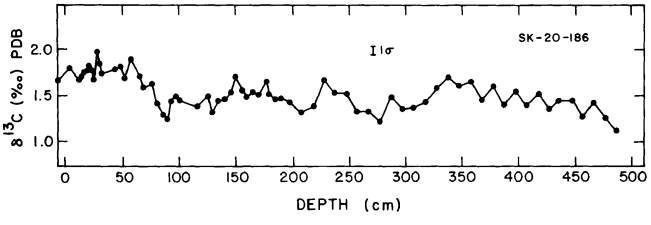

Figure 4. Carbon isotope data of *G. sacculifer* from SK 20-186.

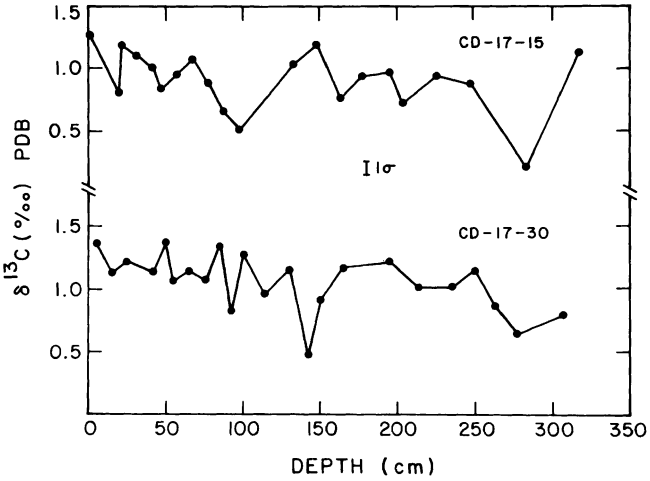

Figure 5. Carbon isotope data *G. sacculifer* from CD 17-15 and CD 17-30.

4.6 *$CaCO_3$ variations and palaeoproductivity*

$CaCO_3$ as percentage of the bulk sediment has been measured in 2 cores SK-20-185 and SK-20-186 (tables 4(a), 4(b) and 6). Along with $CaCO_3$, the coarse fraction (>150 mm), mainly foraminifera, was also measured.

Depth profiles of $CaCO_3$ and the coarse fraction abundances in SK-20-185 are shown in figure 6. $\delta^{18}O$ stages are also shown for the chronological framework. Bold arrows indicate 18 ka level. $CaCO_3$ decreases from Holocene (∼68%) to LGM (∼40%). It increases again to 60% during the interglacial stage 5e. $CaCO_3$ and $\delta^{18}O$ show a negative correlation (∼−0.6), significant at 2.5% level. Major $\delta^{18}O$ stages are also reflected in the $CaCO_3$ profile. In stage 5, however, only two sub-stages are found as against five in $\delta^{18}O$. This is possibly because of the coarser resolution with which $CaCO_3$ was measured below 150 cm depth. The coarse fraction also varies sympathetically with $CaCO_3$ in this core; from 27% in Holocene, it decreases to 5% during LGM. Such a similarity indicates that most of the $CaCO_3$ is mainly biogenic calcite. Considering the depth of the core, dissolution seems to be unlikely to produce these variations in $CaCO_3$ and coarse fraction (Peterson and Prell 1985). The variation, we believe, is due to change in biological productivity through time (Naidu and Malmgren 1995a, 1995b, 1996).

Based on the sedimentation rates derived from ^{14}C and $\delta^{18}O$ stratigraphy and using $CaCO_3$ abundance, the time variation of terrigenous and carbonate fluxes

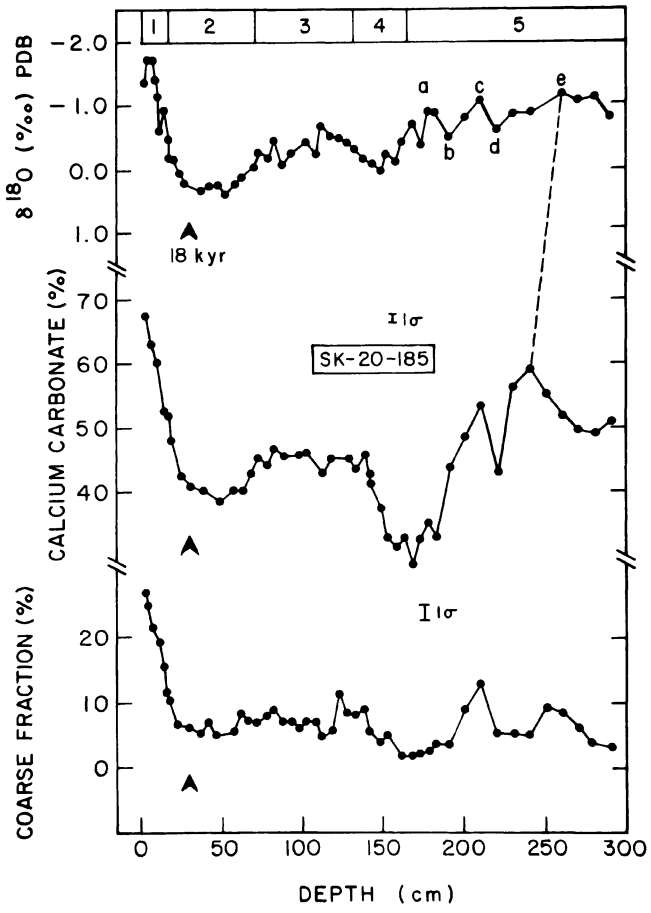

Figure 6. A comparison between oxygen isotope data (*G. sacculifer*), $CaCO_3$ % and coarse fraction % in SK 20-185.

have been calculated for SK-20-185 and are shown in figure 7. For this calculation we have assumed that the density of the sediments varies with the $CaCO_3$ content as shown by Lyle and Dymond (1976); $\rho^{-1} = 0.88 - 0.22\,C - 0.03\,C^2$, where ρ is the density and C is the weight fraction of $CaCO_3$ in the dry sediment. Terrigenous and carbonate fluxes are anticorrelated in this core. Carbonate flux (in $gm\,cm^{-2}\,ka^{-1}$) decreases from Holocene value of 1.02 to 0.62 during LGM, while terrigenous flux increases from 0.49 to 1.05. The lower carbonate flux probably indicates lowering of productivity due to weaker upwelling and summer monsoon conditions during LGM. On the other hand higher terrigenous flux during LGM was probably due to increased rate of erosion when the rivers were cutting across the newly exposed shelf after the lowering of sea level. However, the maximum decrease in productivity and simultaneous increase in terrigenous input took place in stage 4. During the last interglacial (stage 5) productivity was again high, though not as much as during Holocene.

Depth profiles of $CaCO_3$, the coarse fraction and $\delta^{18}O$ in core SK-20-186 are shown in figure 8. In general, the $CaCO_3$ in this core is very high compared with SK-20-185 (~80%). ^{14}C based sedimentation rate and $CaCO_3$ content gives a Holocene carbonate flux of 1.57 gm $cm^{-2}\,ka^{-1}$ at this equatorial region, comparable to sediment trap measurements (Nair *et al* 1989). The terrigenous flux in this core is almost constant (0.1 to $0.3\,gm\,cm^{-2}\,ka^{-1}$) throughout and since the $CaCO_3$ abundance is very high, its variation is taken as an index of productivity. Holocene $CaCO_3$ abundance of ~90% in this core reduces to ~80% during LGM indicating lower productivity. There also exists an apparent negative correlation between $\delta^{18}O$ and $CaCO_3$ in this core, too (shown by dashed lines, figure 8). So by and large, it appears that the LGM was characterized in both Arabian Sea and equatorial Indian Ocean by low biogenic production compared to Holocene. This trend was persistent in the preceding glacial-interglacial cycles as well.

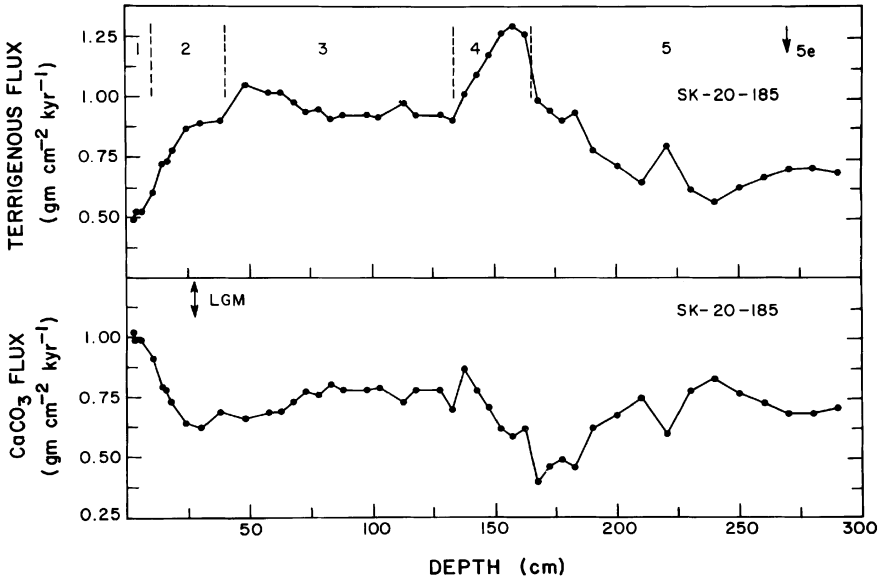

Figure 7. Terrigenous and carbonate fluxes inferred from SK 20-185.

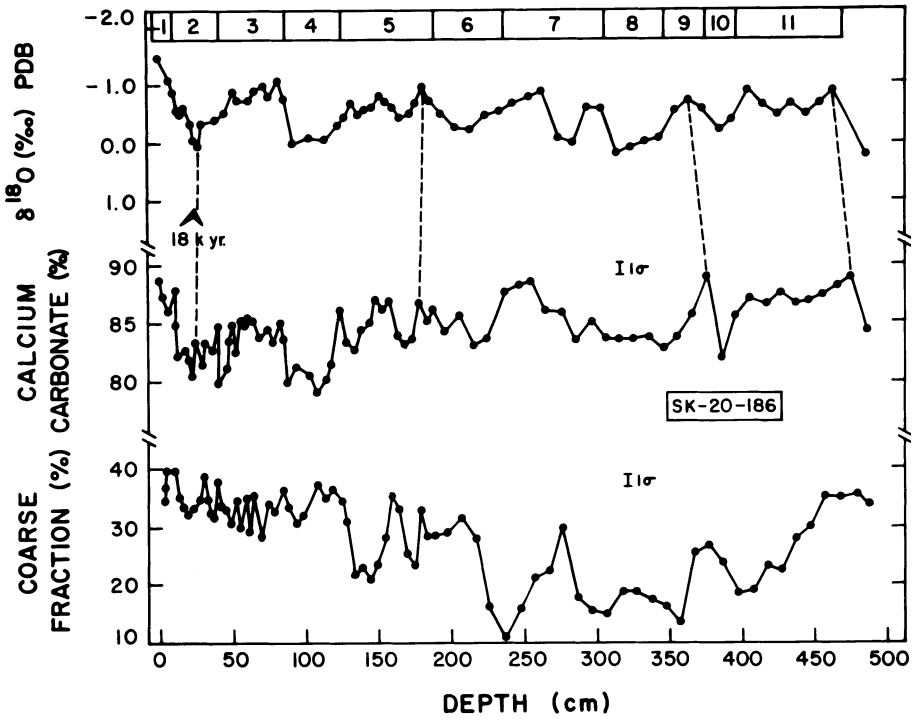

Figure 8. A comparison between oxygen isotope data (*G. sacculifer*), $CaCO_3$ % and coarse fraction % in SK 20-186.

5. Conclusions

$\delta^{18}O$ data from five deep sea cores from the Arabian Sea and the equatorial Indian Ocean provide stratigraphic records ranging from 30 ka to more than 400 ka. During the last glacial-interglacial transition, the Arabian Sea cores in general show a higher $\delta^{18}O$ amplitude than that expected from global ice-volume considerations. This indicates that the Arabian Sea was in general 1 to 2% more saline during the last glacial maximum than at present. The northern Arabian Sea cores show a higher amplitude than the southern ones, whereas the equatorial core shows a lower amplitude. An excess evaporation over the northern Arabian Sea and increased oceanic precipitation in the equatorial Indian Ocean could be responsible for this effect. This was due to the weakening of the summer monsoon during the last glacial period. These results are in agreement with earlier studies (Duplessy 1982; Van Campo *et al* 1982). The weakening of the monsoon led to a reduced upwelling and productivity recorded by $\delta^{13}C$ and $CaCO_3$ abundances. Calculation of the $CaCO_3$ flux shows that the biogenic productivity in the Arabian Sea decreased by ∼65% during LGM relative to Holocene. A similar reduction has also been observed in the equatorial Indian Ocean, though to a lesser extent (∼ 10%). Terrigenous input into the Arabian Sea doubled at the same time possibly due to higher erosion rate along the west coast of India. Around 9 ka the summer monsoon intensified and the effect of enhanced upwelling is seen in the $\delta^{13}C$ of three species of planktonic foraminifera.

Acknowledgements

We thank the ship officers and crew of Sagar Kanya (Cruise # 20) and Charles Darwin (Cruise # 17) for assistance in core collection, M P K Kurup and K K Sivasankaran for technical assistance, S Krishnaswami and B L K Somayajulu for encouragement and the anonymous referees for comments. This work was supported by grants for palaeoclimatic studies from the Department of Science and Technology and Department of Ocean Development, India and NERC, UK.

References

Benn D I and Owen L A 1998 The role of Indian summer monsoon and the mid-latitude westerlies in Himalayan Glaciation: review and speculative discussion; *J. Geol. Soc. London* **155** 353–363.

Bhattacharyya A 1989 Vegetation and climate during the last 30,000 years in Ladakh; *Palaeogeog. Palaeoclim. Palaeoecol.* **73** 25–38

Berger W H, Killingley J S, Metzler C V and Vincent E 1985 Two step deglaciation: ^{14}C dated high resolution $\delta^{18}O$ records from the tropical Atlantic; *Quat. Res.* **23** 258–271

Beufort L, Lancelot Y, Camberlin P, Cayre O, Vincent E, Bassinot F and Labeyrie L D 1997 Insolation cycles as a major control of Equatorial Indian Ocean primary production; *Science* **278** 1451–1454

Broecker W S and Denton G H 1989 The role of ocean-atmosphere reorganizations in glacial cycles; *Geochim. Cosmochim. Acta* **53** 2465–2501

Clemens S, Prell W, Murray D, Shimmield G and Weedon G 1991 Forcing mechanisms of the Indian Ocean Monsoon; *Nature* **353** 720–725

Clemens S and Prell W 1991 Late Quaternary forcing of Indian Ocean summer-monsoon winds: A comparison of Fourier model and General Circulation Model results; *J. Geophys. Res.* **96D12** 22683–22700

Cole J, Fairbanks R, Rind D, Koster R, Thompson L and Mosley-Thompson E 1991 Comparison of a high resolution deuterium record from the Dunde ice cap (Tibetan Plateau) and GCM isotope tracer simulations; *XIII INQUA Congress Abstracts* Beijing China (2–9 August 1991) 63

Duplessy J C, Be A W H and Blanc P L 1981 Oxygen and carbon isotopic composition and biogeographic distribution of planktonic foraminifera in the Indian Ocean; *Palaeogeog. Palaeoclim. Palaeoecol.* **33** 9–46

Duplessy J C 1982 Glacial to interglacial contrasts in the northern Indian Ocean; *Nature* **295** 494–498

Emrich K, Ehhalt D H and Vogel J C 1970 Carbon isotope fractionation during precipitation of calcium carbonate; *Earth Planet. Sci. Lett.* **8** 363–371

Erez J and Luz B 1983 Experimental palaeotemperature equation for planktonic foraminifera; *Geochim. Cosmochim. Acta* **4** 1025–1031

Gote-Ostland H, Craig H, Broecker W S and Spenser D (ed) 1987 *Geosecs Atlantic Pacific and Indian Ocean expeditions* **7** Washington DC: National Science Foundation

Gupta S K, Sharma P and Shah S K 1992 Source of fresh water spike at LGM in the Indian Ocean: An alternative interpretation; *J. Quat. Sci.* **7(3)** 247–255

Gupta S K and Sharma P 1993 Enigma of the negative $\delta^{18}O$ pulse at LGM -a reply; *Curr. Sci.* **65(7)** 514–515

Guptha M V S, Naidu P D and Muralinath A S 1990 Premonsoon living planktonic foraminifera from the south-eastern Arabian Sea; *J. Geol. Soc. India* **36** 654–660

Imbrie J, Hays J D, Martinson D G, Mix A C, Morley J J, Pisias N G, Prell W L, and Shackleton N J 1984 The orbital theory of pleistocene climate: support from a revised chronology of the marine $\delta^{18}O$ record; *Milankovitch and Climate Part-I* (eds) A Berger, J Imkbrie, J D Hays and B Saltzman (Dordrecht: Reidel) 269–305

Kallel N, Labeyrie L D, Juille-Leclere A and Duplessy J C 1988 A deep hydrological front between intermediate and deep water masses in the glacial Indian Ocean; *Nature* **333** 651–655

Krishnamurthy R V 1990 Oxygen in the Arabian Sea; *Nature* **348** 118

Kroopnick P M 1985 The distribution of $\delta^{13}C$ of ΣCO_2 in the world oceans; *Deep Sea Res.* **32** 57–84

Labeyrie L D, Duplessy J C and Blanc P L 1987 Variations in mode of formation and temperature of oceanic deep waters over the past 125,000 yrs; *Nature* **327** 477–482

Lyle M W and Dymond J 1976 Metal accumulation rates in the south east Pacific-errors introduced from assumed bulk densities; *Earth. Planet. Sci. Lett.* **30** 164–168

Mix A C 1987 The oxygen-isotope record of glaciation *The Geology of North America and adjacent oceans during the last deglaciation* **K-3** (Geological Society of America) 111–135

Naidu P D, Rao P S and Pattan J N 1989 Planktonic foraminifera from a Quaternary deep sea core from the southern Arabian Sea; *J. Geol. Soc. India* **34** 393–397

Naidu P D, Babu P C and Rao Ch M 1992 The upwelling record in the sediments of the western continental margin of India; *Deep Sea Res.* **39¾** 715–723

Naidu P D and Malmgren B A 1995a Monsoon upwelling effects on test size of some planktonic foraminiferal species from the Oman Margin, Arabian Sea; *Paleoceanography* **10(1)** 117–122

Naidu P D and Malmgren B A 1995b Do benthic foraminifer records represent a productivity index in oxygen minimum zone areas? An evaluation from the Oman Margin, Arabian Sea; *Marine Micropaleontology* **26** 49–55

Naidu P D and Malmgren B A 1996 A high resolution record of Late Quaternary upwelling along the Oman Margin, Arabian Sea based on planktonic foraminifera; *Paleoceanography* **11(1)** 129–140

Nair R R and Hashimi N H 1980 Holocene climatic inferences from the sediments of the Western Indian continental shelf; *Proc. Indian Acad. Sci.* **89-A** 299–315

Nair R R, Ittekkot V, Manganini S J, Ramaswamy V, Haake B Degens E T, Desai B N and Honjo S 1989 Increased particle flux to the deep ocean related to monsoons; *Nature* **338** 749–751

Naqvi S W A 1993 Enigma of the negative $\delta^{18}O$ pulse at LGM; *Curr. Sci.* **65(7)** 512–514

Naqvi S W A and Fairbanks R G 1996 A 27,000 year record of Red Sea outflow: Implication for the timing of post-glacial monsoon intensification; *Geophys. Res. Lett.* **23(12)** 1501–1504

Pande K, Padia J T, Ramesh R and Sharma K K Stable isotope systematics of surface water bodies in the Himalayan and trans-Himalayan (Kashmir) region; *Proc. Indian Acad. Sci. (Earth Planet. Sci.)* **109**, 109−115

Peterson L C and Prell W L 1985 Carbonate preservation and rates of climatic changes: An 800 kyr record from the Indian Ocean; *The carbon cycle and atmospheric CO_2; Natural Variations Archean to Present* (eds) E T Sandquist and W S Broecker 251–269

Prell W L 1978 Glacial-Interglacial variability of monsoonal upwelling: western Arabian Sea; *International Conference on Evolution of Planetary Atmospheres and Climatology of the Earth* Centre Nice: National d'Etude Spatiales 129–136

Prell W L and Curry W B 1981 Faunal and isotopic indices of monsoonal upwelling: western Arabian Sea; *Oceanologica Acta* **4** 91–98

Prell W L 1984 Monsoonal climate of the Arabian Sea during the late Quaternary: A response to changing solar radiation; *Milankovitch and Climate Pt 1* (eds) A L Berger *et al* (Dordrecht: Riedel) 349–366

Rostek F, Bard E, Beufort L, Sonzogni C and Ganssen G 1997 Sea surface temperature and productivity records for the past 240 kyr in the Arabian Sea; *Deep Sea Res.* **44(6–7)** 1461–1480

Sarkar A and Bhattacharya S K 1988 An on-line CO_2 extraction system for stable isotope analysis of carbonates; *Preprints Volume Fourth National Symposium of Mass Spectrometry* (eds) T R Kasturi *et al* 1–7 Bangalore: Indian Society of Mass Spectrometry 1–3

Sarkar A 1989 Oxygen and carbon isotopes in Indian Ocean sediments and their palaeoclimatic implications; Unpublished PhD thesis, Gujarat University, India

Sarkar A, Ramesh R, Bhattacharya S K and Rajagopalan G 1990a Oxygen isotope evidence for a stronger winter monsoon current during the last glaciation; *Nature* **343** 549–551

Sarkar A, Ramesh R and Bhattacharya S K 1990b Effect of sample pre-treatment and size fraction on the $\delta^{18}O$ and $\delta^{13}C$ of foraminifera in Arabian Sea sediments; *Terra Nova* **2** 489–493

Sarkar A, Bhattacharya S K and Sarin M M 1992 Geochemical evidence for anoxic deep water in the Arabian Sea during the last glaciation; *Geochim. Comochim. Acta* **57** 1009–1016

Shackleton N J and Opdyke N D 1973 Oxygen isotope and palaeomagnetic stratigraphy of equatorial Pacific core V28–238: Oxygen isotope temperatures and ice volumes on a 10^5 year and 10^6 year scale; *Quat. Res.* **3** 35–55

Shackleton N J 1974 Attainment of isotopic equilibrium between ocean water and the benthonic foraminifera genus *Uvigerina*: Isotopic changes in the ocean during the last glacial; *Variation du Climat au Cours du Pleistocene* CNRS Paris 203–209

Sirocko F, Sarnthein M, Erlenkeuser H, Lange H, Arnold M and Duplessy J C 1993 Century scale events in monsoonal climate over the past 24,000 years; *Nature* **364** 322–324

Sirocko F, Schoenberg D G, McIntyre A and Molfino B 1996 Teleconnections between the subtropical monsoons and high latitude climates during the last glaciation; *Science* **272** 526--529

Thompson L G, Mosley-Thompson E, Davis M E, Bolzan J F, Dai J, Yao T, Gundestrup N, Wu X, Klain L and Xie Z, 1989 Holocene-late Pleistocene climatic ice core records from Qunghai-Tibetan Plateau; *Science* **246** 474–477

Van Campo E, Duplessy J C and Rossignol-Strick M 1982 Climatic conditions deduced from a 150 kyr oxygen isotope-pollen record from the Arabian Sea; *Nature* **296** 56–59

Wyrtki K 1971 *Oceanographic Atlas of the International Indian Ocean Expedition* (Washington DC: National Science Foundation)

Wyrtki K 1973 *The Biology of the Indian Ocean* (ed) Zeitschel (New York: Springer) 18–36